The DC1 domain protein Vacuoleless Gametophytes regulates stamen development in Arabidopsis

Natalia L. Amigo[†], Leonardo A. Arias[†], Fernanda Marchetti[†], Sebastián D´Ippólito, Jesica Frik, María Cristina Lombardo, María Cecilia Terrile, Claudia A. Casalongue, Gabriela C. Pagnussat, Diego F. Fiol[*]

Instituto de Investigaciones Biológicas, IIB-CONICET-Universidad Nacional de Mar del Plata, Mar del Plata, Buenos Aires, Argentina.

[†]These authors have contributed equally to this work and share first authorship

[*]Corresponding Author

diefiol@mdp.edu.ar

Key Message. **Vacuoleless Gametophytes is involved in anther dehiscence through a process that involves JA, ROS and lignin accumulation.**

Abstract

Vacuoleless Gametophytes (VLG) is a DC1 domain protein that was initially characterized as essential for early female and male gametophytes development in Arabidopsis. However, VLG expression was also detected in stamens, pistils and other sporophytic tissues, implying a broader role for this protein. As homozygous insertional VLG lines resulted unviable, we generated Arabidopsis amiRNA *VLG* knock-down plants to study the role of VLG in sporophyte development. The phenotypic characterization of *VLG* knock-down plants showed reduced seed set and indehiscent anthers with shorter filaments and stigma exsertion. Moreover, amiRNA *VLG* knock-down plants displayed unbroken stomia and septa, markedly reduced endothecium lignification, diminished ROS accumulation, and lower transcript levels of genes involved in jasmonic acid and lignin biosynthesis. The indehiscent phenotype was rescued by exogenous treatments of either jasmonic acid or H_2O_2. Altogether, our results suggest that VLG is involved in lignin and jasmonic acid biosynthesis pathways, and that proper levels of VLG are required in the process that leads to stomium breakage and anther dehiscence. Our findings shed light on the mechanisms underlying stamen development and provide new insights into the roles of a DC1 domain protein in plant reproduction.

Keywords: anther dehiscence, jasmonic acid, lignin biosynthesis, reactive oxygen species, stamen development

Introduction

Stamen development is a complex and meticulously orchestrated process that is crucial for plant reproduction. It can be broadly divided into early stages, where cell specification occurs, and late stages, where filaments elongate, anther layers are formed (epidermis, endothecium, middle layer and tapetum) and dehiscence of anthers takes place, releasing mature pollen (Wilson et al. 2011). Each of these stages is regulated by a network of genetic and hormonal signals, and any disruption in these processes can lead to male sterility, which has significant implications for crop yield and plant biodiversity (Verma 2019).

Auxin and jasmonic acid (JA) are hormones that play pivotal roles in regulating general floral development, including stamen elongation and anther dehiscence (Cecchetti et al. 2008). Cecchetti et al. (2013, 2017) established that a peak of auxin in the middle layer negatively regulates endothecium lignification and JA biosynthesis, two fundamental processes that precede anther dehiscence. The study of numerous indehiscent mutants has shown that JA regulates the process of stomium breakage, where a specialized group of anther cell layers incur in programmed cell death allowing endothecium expansion and pollen release (Wilson et al. 2011). Moreover, JA synthesized in the upper part of the filaments is thought to regulate water transport from anthers to filaments, resulting simultaneously in anther wall dehydration and filament elongation, both crucial for a timely anthesis (Ishiguro et al. 2001).

Reactive oxygen species (ROS) also play a significant role in stamen development. During anther development, H_2O_2 accumulation induces lignin biosynthetic gene expression (Dai et al. 2019) and is also responsible for catalyzing lignin polymerization in the endothecium (Boerjan et al. 2003). Production of ROS may also play a role in the programmed cell death (PCD) that takes place during both septum and stomium breakage (Kurusu and Kuchitsu 2017).

Vacuoleless Gametophytes (VLG) is a DC1 domain protein required for early gametophytic development (D'ippólito et al. 2017). *VLG* mutants fail to form the central vacuole that is required early in the development of embryo sacs and pollen grains, causing early arrest in both gametophytes (D'ippólito et al. 2017). VLG is localized at the endomembrane system and it was proposed to act as a scaffold protein, as it was proved to interact with a number of proteins including SNARE associated proteins, lipases and transcription factors (D'ippólito et al. 2017). Although VLG function has only been described in gametophytes, *VLG* extensively expresses in the sporophyte, particularly in vasculature and tissues undergoing cellular expansion, which suggests that it may play additional roles in plant development (D'ippólito et al. 2017).

In this work we aimed to study the involvement of VLG during sporophyte development. We generated and analyzed *VLG* knockdown lines and we provided evidence that VLG participates in stamen development in Arabidopsis. We showed that VLG is necessary for correct anther dehiscence, in a pathway that requires JA, ROS accumulation, and lignin biosynthesis. Our findings shed light on the mechanisms underlying stamen development and provide new insights into the roles of VLG in plant reproduction.

Results

VLG knock-down causes reduced seed set, anther indehiscence and impaired anthesis.

VLG is essential for early gametophyte development and the mutant *vlg* phenotype is highly penetrant, making homozygous lines unviable (D'ippólito et al. 2017). Therefore, to assess VLG function in the sporophyte, we constructed knock-down transgenic lines expressing *pro35S:amiRNA* (amiR-VLG) to specifically target and knock-down *VLG* transcripts. We analyzed VLG expression in inflorescences of three independent amiR-VLG lines (L1, L2 and L3) and found that *VLG* transcripts were reduced about 65%, 75% and 85% in L1, L2 and L3 respectively, as compared to WT plants (Fig. 1A).

amiR-VLG plants developed normally until flowering, except for minor differences in rosette leaves, which displayed an epinastic phenotype (curved towards their abaxial side) under normal growth conditions (Fig. 1B, C). At flowering, all three amiR-VLG lines consistently presented shorter siliques with few to no seeds. As it can be seen in Fig. 1D, E, this phenotype was more marked in the first 8-10 siliques and become less pronounced as the plants aged.

To better assess the causes of the reduced seed set, we performed a morphological characterization of floral structures. Flowers from amiR-VLG plants were similar to WT flowers regarding opening time, sepals, petals and development of stigmatic papillae, However, amiR-VLG flowers presented indehiscent anthers, significantly shorter stamen filaments (around 12% shorter than filaments from WT plants) and longer pistils (about 19% longer than pistils from WT plants), resulting in a substantially higher pistil/stamen length ratio that likely hinders pollination (Fig.1F-I).

To inspect the cause of the amiR-VLG-related indehiscent phenotype, we analyzed transverse sections of anthers during anthesis (stage 14). As opposed to WT anthers, amiR-VLG anthers do not show septa and stomia breakage (Supplementary Fig. S1). Additionally, indehisced anthers also appear collapsed, suggesting a weak secondary wall structure (Supplementary Fig. S1).

VLG is expressed throughout flower development

In order to assess whether *VLG* could be involved in flower development, we analyzed the expression profile of *proVLG:GUS* reporter lines. *VLG* promoter activity is detectable all along the flower development process (Fig. 2). During the early stages of flower buds, from stages S1 to S10 (according to Smyth et al., 1990), the expression occurs in all flower organs (Fig. 2B-F). However, as the flower matures, it becomes more localized to the anthers, stamen filaments, and style (Fig. 2 G-P).

VLG knock-down lines show impaired lignification and reduced H_2O_2 accumulation in anthers

Several anther indehiscent phenotypes have been reported in the literature, either caused by impaired endothecium lignification (Cecchetti et al. 2013) or reduced H_2O_2 accumulation (Dai et al. 2019).

To analyze endothecium lignification, we used confocal microscopy to analyze anthers stained with ethidium bromide and acridine orange to highlight lignin and cellulose respectively. We observed a very significant reduction of lignin content in anthers from amiR-VLG lines L1 and L2, while in amiR-VLG L3 anthers lignin staining was only slightly lower as compared to the WT (Fig. 3B). Moreover, acridine orange staining evidenced that the shape of endothecium cells in amiR-VLG lines was heavily distorted (Fig 3B). WT cells are roughly even in size and present an orthogonal shape with a wide contact surface between cell walls. On the other hand, amiR-VLG endothecium cells are highly irregular in size, rounder, and display narrow contact surfaces (Fig. 3B). That was especially evident for L1 and L2, which presented the lowest lignin contents.

To assess if H_2O_2 accumulation is involved in the reduced lignification observed, we used diaminobenzidine (DAB) staining on whole anthers from WT and amiR-VLG plants. We examined anthers between stages S11 and S13, as these stages were reported to be relevant for H_2O_2 accumulation by Dai et al. (2019). Interestingly, we found a marked decrease in H_2O_2 accumulation in all three amiR-VLG lines, showing DAB staining values about one-third lower compared to WT anthers (Fig. 3C, D).

amiR-VLG anther indehiscent phenotype is rescued by both MeJA and H_2O_2 exogenous treatments

In previous studies, authors have been able to rescue indehiscent anthers by exogenous applications of JA (Wilson et al. 2011) or H_2O_2 (Dai et al. 2019).

In order to test if amiR-VLG indehiscent lines were defective in a pathway dependent on JA or H_2O_2, we applied MeJA (1 mM), JA (0.5 mM) or H_2O_2 (1 mM) by briefly immersing inflorescences in either solution once a day for three consecutive days. Strikingly, each treatment independently

restored correct anther dehiscence in all three lines, resulting in proper fruit development with a complete seed set (Fig. 4, Supplementary Fig. S2, S3). These results suggest that VLG is required to maintain proper levels of JA and H_2O_2 in anthers. In contrast, none of these treatments reverted the short filaments nor the long pistil phenotypes of amiR-VLG lines, even when anther dehiscence was indistinguishable from WT plants (Fig. 4A, B, E, F, Supplementary Fig. S2, S3).

Knock-down of *VLG* reduces the expression levels of JA and lignin biosynthetic genes

As amiR-VLG lines displayed phenotypes consistent with impaired lignin and JA biosynthesis, we analyzed the expression of key genes belonging to those pathways in inflorescences from WT and from amiR-VLG lines.

Thus, we measured transcript abundance through RT q-PCR of *SND2* (*Secondary wall-associated NAC Domain 2, NAC073*), a gene that encodes a transcription factor that regulates the expression of genes involved in secondary cell wall development (Zhong et al. 2008), three cellulose biosynthesis genes: *CESA4* (*Cellulose synthase A 4*) (Richmond and Somerville 2000) and two genes of the Irregular Xylem (IRX) family, *IRX3*, and *IRX12* (Hussey et al. 2011). We found significantly lower transcript levels in these four genes in the three amiR-VLG lines compared to WT plants (Fig. 5A-D), supporting the hypothesis that the right levels of *VLG* are necessary for proper lignin biosynthesis.

In addition, we determined the abundance of two gene transcripts involved in JA biosynthesis, *DAD1 (Defective in Anther Dehiscence 1*) which encodes a lipolytic enzyme that catalyzes the synthesis of linolenic acid, in the initial step in the JA biosynthetic pathway (Tabata et al. 2010) and *AOS* (*Allene Oxide Synthase*, *CYP74A*) which encodes a cytochrome P450 enzyme that catalyzes the dehydration of hydroperoxide to an unstable allene oxide in the same pathway (Park et al. 2002). We also found significantly lower transcript levels of these two genes in the three amiR-VLG lines compared to WT plants (Fig. 5E, F), suggesting that *VLG* might be involved in the regulation of the JA biosynthetic pathway.

Discussion

In this work we studied the role of VLG in the sporophytic development of Arabidopsis and found that it is required for the proper development of the stamen. Knocking down *VLG* via amiRNA led to anther indehiscence, short filaments and stigma exsertion, causing a drastic decrease in the seed set (Fig. 1). Using lines carrying the *proVLG:GUS* reporter, we showed that *VLG* is expressed throughout all the developmental stages of the flower, exhibiting strong expression levels in

filaments and during early stages of anther development (Fig. 2). This expression pattern, coupled with the male sterility phenotype observed in amiR-VLG lines, suggests that VLG may play a role in the processes of filament elongation and anther dehiscence.

For successful fertilization, flowers must undergo a series of developmental events in a timely manner. These events include the development of the pistil and stigmatic papillae, the growth of stamens, and the opening of anthers to release pollen. These events are regulated by a combination of genetic, hormonal, and environmental factors. The accurate and timely dehiscence of anthers relies on several key steps, including the development of the four anther cell layers, endothecium lignification, tapetum degeneration, and the opening of septa and stomia (Wilson et al. 2011). The regulation of endothecium lignification is governed by both hormonal control and ROS balance. Between floral stages 10 and 11, an auxin peak negatively regulates endothecium lignification via MYB26, a master activator of cell wall secondary thickening (Cecchetti et al. 2013). In fact, auxin suppresses NAC family transcription factors SND1/2, which directly target and induce MYB26 (Xiao et al. 2021). The early auxin peak also negatively regulates JA biosynthesis by inducing ARF6/8 transcription factors, which indirectly inhibit DAD1, the initial enzyme in the JA biosynthetic pathway (Tabata et al., 2010), ultimately leading to stomium breakage.

We performed transverse sections of anthers before anthesis, revealing the absence of septum and stomium rupture and an apparent lack of endothecium lignification, and confirmed also decreases in lignin and cellulose contents in the amiR-VLG plants (Supplementary Fig. S1, Fig. 3).

The breakage of the stomium is triggered by JA. In most JA biosynthesis mutants, the absence of stomium breakage phenotype can be reversed by MeJA application (Wilson et al., 2011). In agreement with a possible role for VLG regulating JA levels in anthers, we successfully rescued the indehiscent phenotype of amiR-VLG plants with applications of MeJA or JA (Fig. 4, Supplementary Fig. S3).

To ascertain whether the JA biosynthesis pathway was affected in amiR-VLG lines, we quantified two transcripts of the JA biosynthetic pathway, *DAD1* and *AOS*, and observed a significant reduction in the abundance of both transcripts in flower buds from the three amiR-VLG lines (Fig. 5E, F). Thus, we infer that the phenotype of indehiscent anther observed in amiR-VLG lines is consistent with the downregulation of certain genes involved in JA biosynthesis, resulting in a deficiency of JA levels necessary for anther opening.

Therefore, we infer that the phenotype of indehiscent anther observed in amiR-VLG lines is consistent with the downregulation of genes involved in JA biosynthesis, resulting in a deficiency of

JA levels which in turn are necessary for anther opening. Concordantly, previous studies have shown that reduced expression of AOS and DAD1 can lead to male sterility by blocking JA synthesis (Park et al. 2002, Sanders et al. 2000).

Proper levels of H_2O_2 are essential for lignin accumulation in the endothecium, as H_2O_2 induces lignin biosynthetic genes and it is also directly involved in lignin polymerization (Boerjan et al. 2003, Dai et al. 2019). We observed that amiR-VLG plants presented reduced ROS accumulation in anthers (Fig. 3C) and exogenous application of H_2O_2 on floral buds successfully restored proper stomium breakage (Fig. 4E), suggesting that VLG could also be regulating H_2O_2 accumulation. Moreover, amiR-VLG inflorescences also presented a decrease in transcript levels of genes involved in primary and secondary cell wall biosynthesis. We found that the NAC family transcription factor SND2 and genes that encode for its secondary wall thickening-related targets (CESA4, IRX3, and IRX12) were significantly downregulated in VLG knock-down plants (Fig. 5A-E).

Remarkably, SND2 was previously reported as a VLG interacting protein, as detected by a yeast two-hybrid assay (D'ippólito et al. 2017), suggesting that VLG could also participate in the lignin biosynthetic process by interacting with the master regulator gene of secondary thickening. Interestingly, the interaction between another DC1 protein (binucleate pollen, BNP) and two other NAC family transcription factors (Vascular Plant One-Zinc Finger 1 and 2, VOZ1/2) was recently reported (Arias et al. 2022). In this case, it was proposed that BNP, which is localized as VLG in the endomembrane system, was required for a timely nuclear translocation of VOZ1/2 during pollen development (Arias et al. 2022).

VLG knock-down plants treated with either JA, MeJA or H_2O_2 did not recover the short filament phenotype (Fig. 4, Supplementary Fig. S2, S3). Filament elongation is hypothesized to rely upon JA synthesized in the upper regions of the filaments, which regulates water transport from the anthers to the filaments (Ishiguro et al. 2001). However, this process appears to be uncoupled from anther dehiscence (Cecchetti et al. 2008). Therefore, the timing and concentrations of exogenous applications required to rescue those phenotypes may differ substantially. During the late phase of stamen development, others molecules, such as auxins, play a crucial role in controlling the process. For instance, the maximum concentration of auxin is established in the anthers at the beginning of the stage (stage 10). This triggers filament elongation and negatively controls anther dehiscence and pollen maturation. As tapetum degenerates, the concentration of auxin decreases. Misregulation in the occurrence or in the timing of the components involved in the anther development process can lead to a reduced seed set in amiR-VLG lines. To better understand the involvement of this important

hormone in the process, a study of auxin distribution in different stages of stamen development in VLG mutants will be necessary.

Based on these findings and existing literature, we propose a model wherein VLG modulates the expression of JA biosynthesis genes, leading to timely stomium breakage. VLG is also involved upstream H_2O_2 accumulation in anthers around flower stage 11. The peak of H_2O_2 in turn induces lignin biosynthesis gene expression, resulting in proper endothecium lignification. A possible way of action of VLG in the lignin biosynthesis pathway could be through the interaction with SND2, the secondary wall thickening master regulator. Deficient VLG levels in amiR-VLG stamens could impair the formation of molecular complexes required for JA biosynthesis, H_2O_2 accumulation and lignin biosynthesis required for proper anthesis. Follow-up work will be aimed to identify the proteins interacting with VLG in this process.

Materials and Methods

Plant materials and growth conditions

Arabidopsis thaliana ecotype Columbia (Col-0) WT and knock-down plants were grown in growth chambers under long-day conditions (16-h light/8-h dark) at 25°C and 50-70% humidity. Seeds were treated in 50% (v/v) sodium hypochlorite with 0.1% Tween-20, washed five times with sterile water, stratified at 4°C for 48 h and plated on Murashige and Skoog media, with 50 µg/ml kanamycin and/or 50 µg/ml hygromycin when necessary, at the light and temperature conditions indicated above. Resistant seedlings were subsequently moved from plates to soil. Arabidopsis plants were transformed using the floral dip method (Clough and Bent 1998) with the *Agrobacterium tumefaciens* strain GV3101. proVLG:GUS plants were previously reported by (D'ippólito et al. 2017), The numerical designation of developing flower buds was adopted according to (Smyth et al. 1990).

Knock-down of *VLG*

VLG knock-down plants were generated using an artificial microRNA (amiR) strategy described in (Schwab et al. 2010). Primers listed in Supplementary Table S1 were designed using Web MicroRNA Designer (WMD3, http://wmd3.weigelworld.org/cgi-bin/webapp.cgi) tools to incorporate a 21-bp amiRNA sequence into the MIR319a vector. Subsequently, the amiRNA construct was subcloned into the expression vector pCHF3. The resulting amiR-VLG construct was transformed into Arabidopsis as indicated in the previous section and independent lines were selected (VLG-amiRNA L1-L3).

Morphological and histological analyses

Flowers were collected before anthesis and dissected and cleared in Hoyer's solution or 90% ethanol overnight. After clearing, inflorescences and anthers were observed on a Zeiss Axioplan Imager-A2 microscope under differential interference contrast (DIC) optics. Images were captured on an Axiocam HRC CCD camera (Zeiss, http://www.zeiss.com/) using the Axiovision program (version 4.2). For GUS staining, collected proVLG:GUS developing seedlings and inflorescences were processed as described by (Pagnussat et al. 2007).

Light and confocal microscopy and lignin detection

Inflorescences were fixed in a solution of ethanol:water:phormol:acetic acid (10:7:2:1) and then dehydrated and included in Paraplast (Sigma) according to (de Argüeso 1986, Ruzin 1999). Samples were mounted and cut in a rotary microtome. The sections were stained with Toluidin Blue O and were examined by bright field microscopy in a Nikon Eclipse E 2000 microscope (Tokyo). Images were obtained with a digital camera (Nikon Coolpix 990).

Confocal microscopy was performed using a BX61-FV300 microscope (Olympus Optical, Tokyo, Japan) with an ethidium bromide/acridine orange stain, according to (Yang et al. 2007). Images from the anthers were analyzed by using Image J software (Fiji v.2.15.0).

In situ determination of reactive oxygen species

Detection of hydrogen peroxide (H_2O_2) in plant tissues was performed by DAB staining according to (Villarreal et al. 2009). Briefly, inflorescences of Arabidopsis plants were incubated overnight in total darkness with a DAB solution (0.5 mg/ml) of 3,30-diaminobenzidine (Sigma) in 50 mM sodium acetate buffer (pH 5, 4) at 25°C. Afterward, the solution was removed and samples were decolored with 90% ethanol overnight at 25°C to remove chlorophyll. A dark brown color was visualized for H_2O_2 due to the oxidization of DAB. Images were taken with a binocular SMZ800 (Nikon) and a CoolSnap Pro camera (MediaCybernetics, TX). The DAB signal was digitally quantified as the average pixel light value of about 40 anthers from each condition using Image J software (Fiji v.2.15.0).

RNA isolation and qPCR analysis

Total RNA was extracted from inflorescences with TRIzol reagent (Invitrogen, USA). The amount and quality of RNA were checked by spectrophotometry (OD: 260/280) and by electrophoresis in agarose gels. cDNA was obtained from 1 µg of total RNA pretreated with DNase I (Promega) by reverse transcription reaction using ImProm-II(TM) Reverse Transcriptase (Promega) with random hexamers primers. q-PCR reactions were performed using FastStart Universal SYBR® Green Master (ROX) PCR mix (Roche) in a StepOne machine (Applied Biosystems). The amplification conditions were 95°C for 10 min, followed by 40 cycles of amplification (95°C for 15 s, 60°C for 30 s) and

reactions were conducted in triplicates. Data presented are normalized to the expression level of the control gene actin2 of three independent experiments Sequences of the primers used are listed in Supplementary Table S2. The 'delta–delta Ct method' was used to calculate the relative expression of the genes (Livak and Schmittgen 2001).

Application of methyl jasmonate (MeJA), jasmonate (JA) and H_2O_2

All opened flowers (after stage 14) were removed from the inflorescence, and the remaining flower bud clusters were dipped into 1mM MeJA (Sigma-Aldrich) 500 uM JA (Sigma-Aldrich) or 1mM H_2O_2 dissolved in 0.05% aqueous Tween-20 as indicated in (Shih et al. 2014). The plants were then grown in a growth room under a long day (16/8 h, light/dark) photoperiod at 25°C for 40-50 days. The development of the silique for MeJA, JA or H_2O_2 treated flower buds was recorded and pictures were taken 10 days and 30 days after treatment.

Statistical analysis

Independent experiments were conducted at least two times and assays were performed at least in triplicate. The values obtained were used for statistical analysis between groups using GraphPad Prism, version 6.01. Statistical differences between groups were calculated by applying the Student's t-test or analysis of variance test; and Tukey's or Dunnett's multiple comparisons test were performed, considering $P < 0.05$ as significant.

Funding

This work was supported by grants to DFF from Agencia Nacional de Promoción Cientifica y Técnica Argentina (PICT2017-0232, PICT2021-0185), Consejo Nacional de Investigaciones Cientificas y Técnicas, Comisión de Investigaciones Cientificas (CIC-PBA) and Universidad Nacional de Mar del Plata; a grant to GCP from the Howard Hughes Medical Institute (IECS award 55007430).

Acknowledgments

We would like to thank Viviana Daniel for technical assistance with confocal microscopy.

Figure Legends

Fig. 1. Analysis of amiR-VLG plants. A) Relative quantification of VLG transcripts in inflorescences of WT plants and three independent amiR-VLG lines L1, L2 and L3. 42-day-old plants (**B**) and 26-day-old rosettes (**C**) of WT and amiR-VLG lines (L1, L2 and L3). Bars: 10 mm (in B) and 50 mm (in C). Collection of main stem siliques displayed in chronological order, from the earliest ones in the younger plant to the latest ones in the older plant (**D)** and silique lengths (**E)** of WT plants and amiR-VLG lines L1, L2 and L3. Bar: 10 mm. Flowers at stage S15 (according to

Smyth et al., 1990) (**F**), and their corresponding pistil length (**G**), stamen length (**H**), and ratio of pistil/stamen (**I**) from WT plants and amiR-VLG lines L1, L2 and L3. Scale bar, 10mm. Asterisks indicate significant difference compared to WT plants. ANOVA and Dunnett's multiple comparisons test, $p<0.001$ (***), $p < 0.0001$ (****).

Fig. 2. *VLG* promoter activity in inflorescences. (**A**) GUS signal was detected in inflorescences from 5-week-old proVLG:GUS plants. Different stages of inflorescence are indicated: (**B**) stages S1 to S8, (**C-D**) stage S9, (**E-F**) stage S10, (**G-H**) stage S11, (**I-J**), stage S12, (**K**) stage S13, (**L-M**) stage S14, (**N-O**) stage S15, (**P**) stage S16. Three independent transgenic lines were used for this study. Pictures are representative of the results obtained in all analyzed lines. Scale bars: A, 5 mm; B-K, 0.5 mm; L-P, 1 mm.

Fig. 3. Anther development is affected in amiR-VLG lines. (**A**) Detection of lignin distribution in anthers at stages S11-S13 from WT plants and amiR-VLG lines (L1, L2 and L3) stained with ethidium bromide (EthBr, upper panels) and acridine orange (AcrOrg, lower panels). Bar: 10 µm. ROS accumulation (**B**) and quantification (**C**) in anthers at stages S11-S13 from WT plants and amiR-VLG (L1) were analyzed by DAB staining. Bar: 0.1 mm. Student's t test, $p < 0.0001$ (****).

Fig. 4. Indehiscence of anthers is rescued by Methyl Jasmonate (MeJA) and H_2O_2 exogenous application in amiR-VLG plants. Flowers in 4-week-old plants were treated with 1 mM MeJA (**A-D**) or 1mM H_2O_2 (**E-H**) for three days. The ratio of pistil/stamen (**B**, **F**) and silique length (**D**, **H**) were measured after five and fourteen days post treatments respectively. Arrows indicate the treatment starting point. Bar: 10 mm. B, D, F, H. Asterisks indicate significant differences compared to WT control plants. ANOVA and Dunnett's multiple comparisons test, $p<0.05$ (*), $p < 0.0001$ (****).

Fig. 5. Transcript levels from lignin and JA biosynthesis pathways are affected in amiR-VLG lines. Total RNA was isolated from inflorescences of 5-week-old WT and amiR-VLG lines L1, L2 and L3 and relative transcript levels were calculated. Genes from lignin biosynthesis pathway (**A**) *SND2: Secondary wall-associated NAC Domain 2*, (**B**) *CESA4: Cellulose synthase A4*, (**C**) *IRX3: Irregular Xylem 3*, and (**D**) *IRX12: Irregular Xylem 12* were analyzed. Genes from JA biosynthesis pathway (**E**) *DAD1*: *Defective in Anther Dehiscence 1* and (**F**) *AOS*: *Allene Oxide Synthase*, were analyzed. Data are means of three replicates with ± SD. Asterisks indicate significant differences in comparison to WT plants by ANOVA and Dunnett's multiple comparisons test, $p<0.05$ (*), $p<0.01$ (**), $p<0.001$ (***), $p < 0.0001$ (****).

References

Arias LA, D'Ippólito S, Frik J, Amigo NL, Marchetti MF, Casalongué CA, Pagnussat GC, Fiol DF, 2022. The DC1 Domain Protein BINUCLEATE POLLEN is Required for POLLEN Development in Arabidopsis thaliana. Plant Cell. Physiol. 63, 1994-2007

Boerjan W, Ralph J, Baucher M, 2003. Lignin Biosynthesis. Ann. Rev. Plant. Biol. 54, 519-546.

Cecchetti V, Altamura MM, Brunetti P, Petrocelli V, Falasca G, Ljung K, Costantino P, Cardarelli M, 2013. Auxin controls Arabidopsis anther dehiscence by regulating endothecium lignification and jasmonic acid biosynthesis. Plant J. 74, 411-422.

Cecchetti V, Altamura MM, Falasca G, Costantino P, Cardarelli M, 2008. Auxin regulates Arabidopsis anther dehiscence, pollen maturation, and filament elongation. Plant Cell. 20, 1760-1774.

Cecchetti V, Celebrin D, Napoli N, Ghelli R, Brunetti P, Costantino P, Cardarelli M, 2017. An auxin maximum in the middle layer controls stamen development and pollen maturation in Arabidopsis. New Phytol. 213, 1194-1207.

Clough SJ, Bent AF, 1998. Floral dip: a simplified method for Agrobacterium□mediated transformation of Arabidopsis thaliana. Plant J. 16, 735-743.

D'ippólito S, Arias LA, Casalongué CA, Pagnussat GC, Fiol DF, 2017. The DC 1□domain protein VACUOLELESS GAMETOPHYTES is essential for development of female and male gametophytes in Arabidopsis. Plant J. 90, 261-275.

Dai S-Y, Hsu W-H, Yang C-H, 2019. The gene ANTHER DEHISCENCE REPRESSOR (ADR) controls male fertility by suppressing the ROS accumulation and anther cell wall thickening in Arabidopsis. Sci. Reports. 9, 5112.

de Argüeso ADA, 1986. Manual de técnicas en histología vegetal. Hemisferio Sur

Hussey SG, Mizrachi E, Spokevicius AV, Bossinger G, Berger DK, Myburg AA, 2011. SND2, a NAC transcription factor gene, regulates genes involved in secondary cell wall development in Arabidopsis fibres and increases fibre cell area in Eucalyptus. BMC Plant Biol. 11, 173.

Ishiguro S, Kawai-Oda A, Ueda J, Nishida I, Okada K, 2001. The DEFECTIVE IN ANTHER DEHISCENCE1 gene encodes a novel phospholipase A1 catalyzing the initial step of jasmonic acid biosynthesis, which synchronizes pollen maturation, anther dehiscence, and flower opening in Arabidopsis. Plan tCell 13, 2191-2209.

Kurusu T, Kuchitsu K, 2017. Autophagy, programmed cell death and reactive oxygen species in sexual reproduction in plants. J. Plant Res. 130, 491-499.

Livak KJ, Schmittgen TD, 2001. Analysis of relative gene expression data using real-time quantitative PCR and the 2(-Delta Delta C(T)) Method. Methods. 25, 402-408.

Pagnussat GC, Yu H-J, Sundaresan V, 2007. Cell-fate switch of synergid to egg cell in Arabidopsis eostre mutant embryo sacs arises from misexpression of the BEL1-like homeodomain gene BLH1. Plant Cell. 19, 3578-3592.

Park J-H, Halitschke R, Kim HB, Baldwin IT, Feldmann KA, Feyereisen R, 2002. A knock-out mutation in allene oxide synthase results in male sterility and defective wound signal transduction in Arabidopsis due to a block in jasmonic acid biosynthesis. Plant J. 31, 1-12.

Richmond TA, Somerville CR, 2000. The cellulose synthase superfamily. Plant Physiol. 124, 495-498.

Ruzin SE, 1999. Plant microtechnique and microscopy. Oxford University Press New York

Schwab R, Ossowski S, Warthmann N, Weigel D, 2010. Directed Gene Silencing with Artificial MicroRNAs. Methods in molecular biology (Clifton, NJ) 592, 71-88.

Shih C-F, Hsu W-H, Peng Y-J, Yang C-H, 2014. The NAC-like gene ANTHER INDEHISCENCE FACTOR acts as a repressor that controls anther dehiscence by regulating genes in the jasmonate biosynthesis pathway in Arabidopsis. J. Exp. Bot. 65, 621-639.

Smyth DR, Bowman JL, Meyerowitz EM, 1990. Early flower development in Arabidopsis. Plant Cell 2, 755-767.

Tabata R, Ikezaki M, Fujibe T, Aida M, Tian C-e, Ueno Y, Yamamoto KT, Machida Y, Nakamura K, Ishiguro S, 2010. Arabidopsis auxin response factor6 and 8 regulate jasmonic acid biosynthesis and floral organ development via repression of class 1 KNOX genes. Plant Cell Physiol. 51, 164-175.

Verma N, 2019. Transcriptional regulation of anther development in Arabidopsis. Gene 689, 202-209.

Villarreal F, Martín V, Colaneri A, González-Schain N, Perales M, Martín M, Lombardo C, Braun H-P, Bartoli C, Zabaleta E, 2009. Ectopic expression of mitochondrial gamma carbonic anhydrase 2 causes male sterility by anther indehiscence. Plant Mol. Biol. 70, 471-485.

Wilson ZA, Song J, Taylor B, Yang C, 2011. The final split: the regulation of anther dehiscence. J. Exp. Bot. 62, 1633-1649.

Xiao R, Zhang C, Guo X, Li H, Lu H, 2021. MYB transcription factors and its regulation in secondary cell wall formation and lignin biosynthesis during xylem development. Intl. J. Mol. Sci. 22, 3560.

Yang C, Xu Z, Song J, Conner K, Vizcay Barrena G, Wilson ZA, 2007. Arabidopsis MYB26/MALE STERILE35 regulates secondary thickening in the endothecium and is essential for anther dehiscence. Plant Cell 19, 534-548.

Zhong R, Lee C, Zhou J, McCarthy RL, Ye Z-H, 2008. A Battery of Transcription Factors Involved in the Regulation of Secondary Cell Wall Biosynthesis in Arabidopsis. Plant Cell 20, 2763-2782.

Figure 1

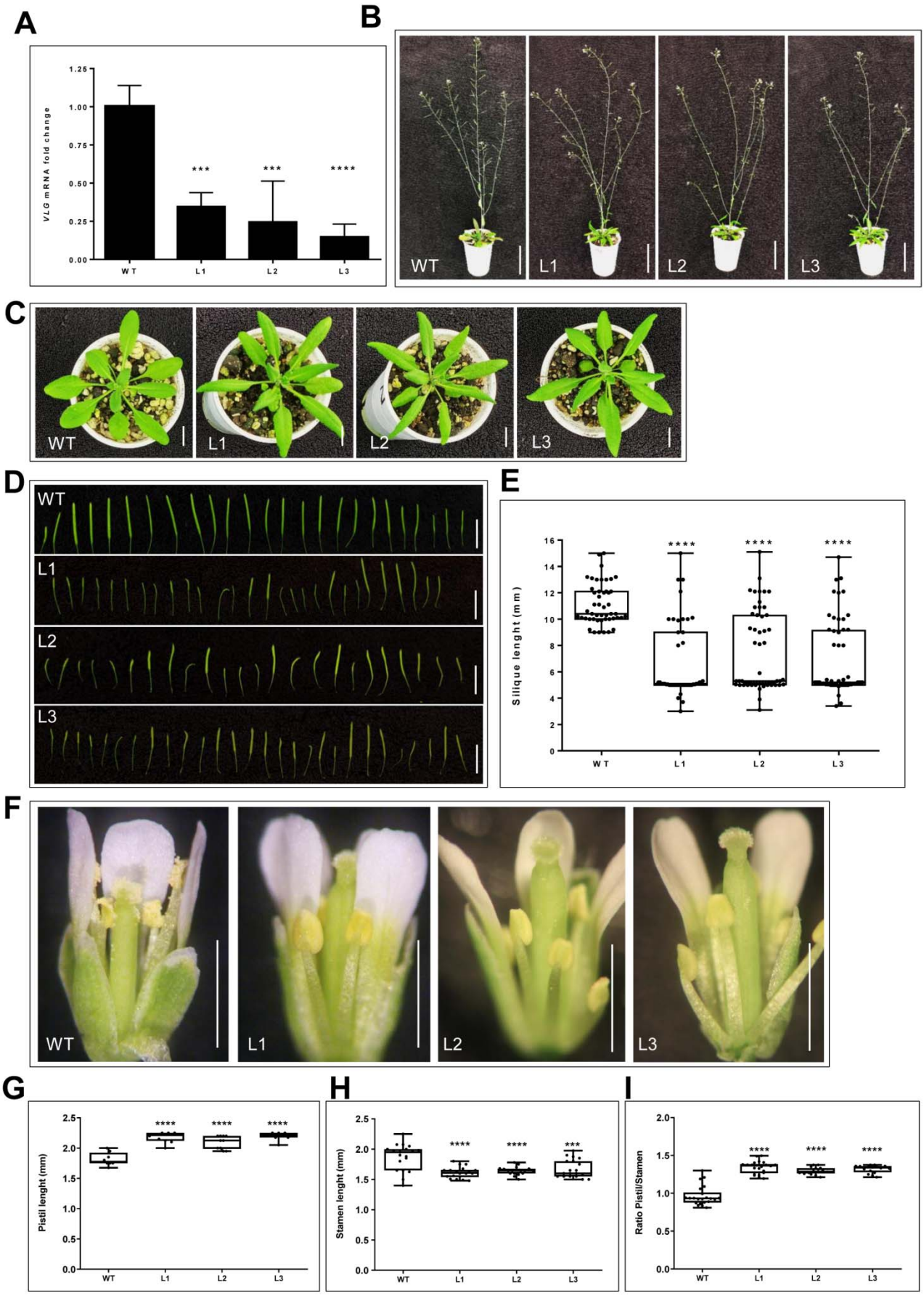
A
B
C
D
E
F
G
H
I
VLG mRNA fold change
WT
L1
L2
L3
Silique lenght (mm)
Pistil lenght (mm)
Stamen lenght (mm)
Ratio Pistil/Stamen

Figure 2

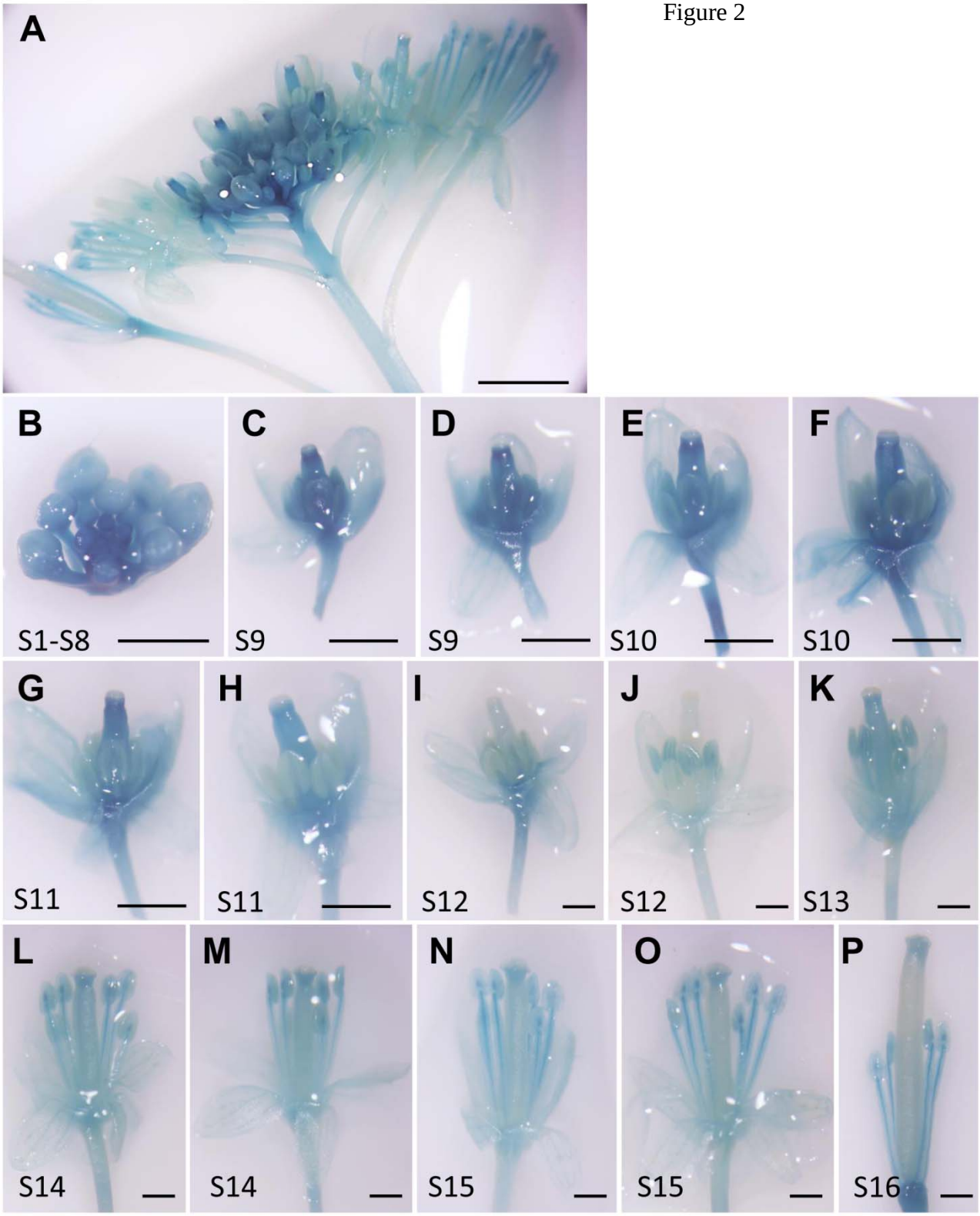
A
B
S1-S8
C
S9
D
S9
E
S10
F
S10
G
S11
H
S11
I
S12
J
S12
K
S13
L
S14
M
S14
N
S15
O
S15
P
S16

Figure 3

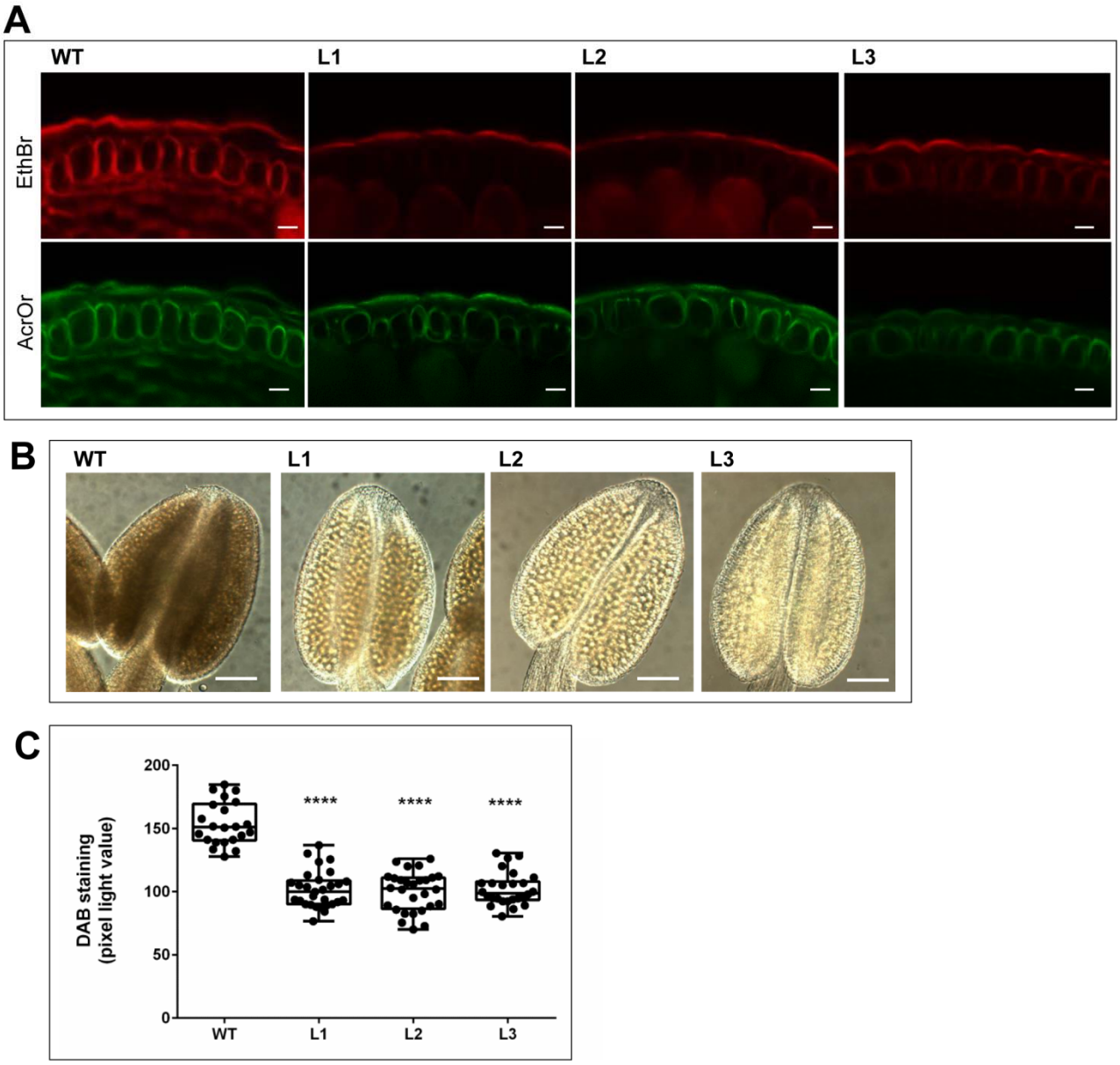
A
WT
L1
L2
L3
EthBr
AcrOr
B
WT
L1
L2
L3
C
DAB staining
(pixel light value)
200
150
100
50
0
****
****
****
WT
L1
L2
L3

Figure 4

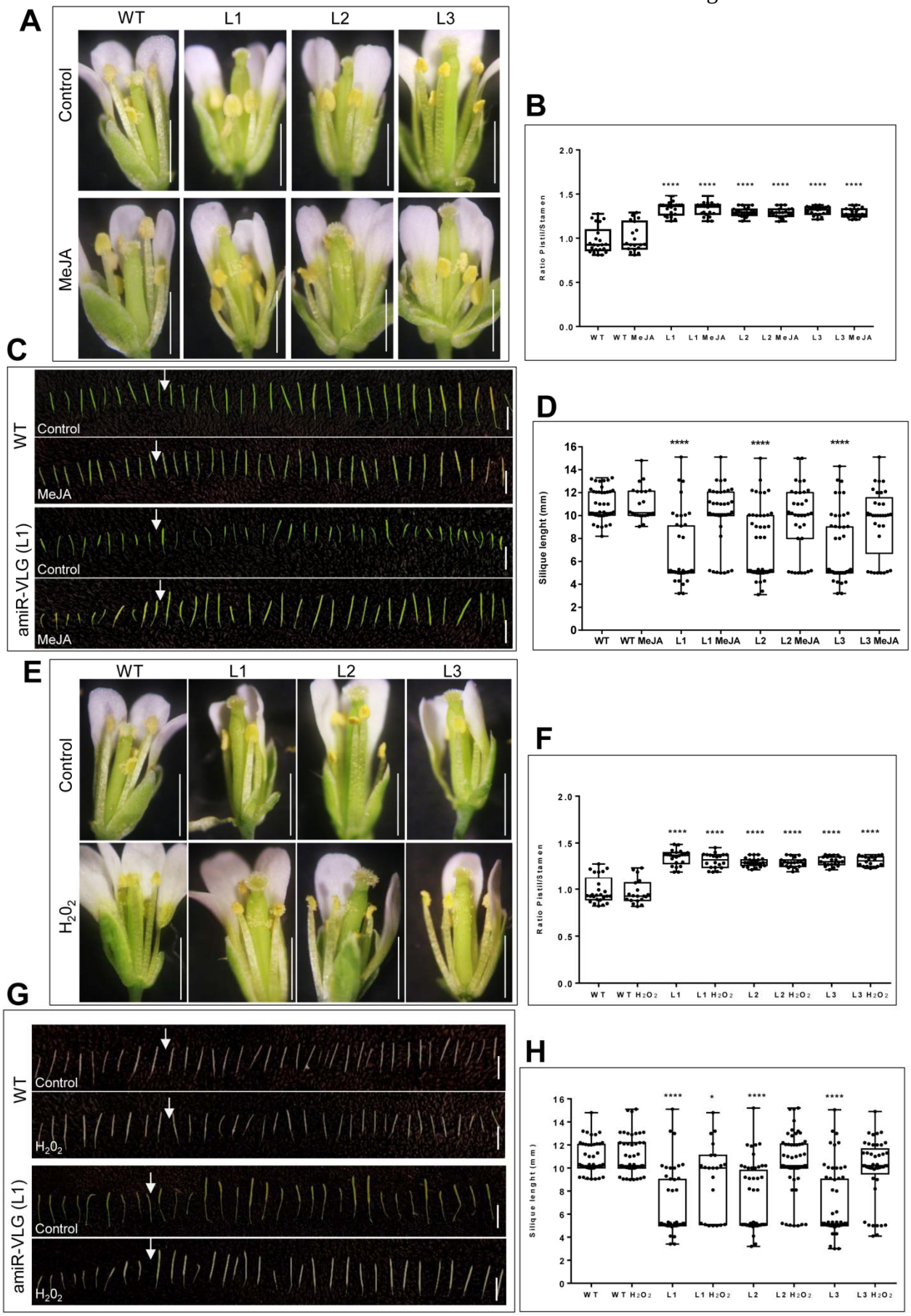
A
WT
L1
L2
L3
Control
MeJA
B
Ratio Pistil/Stamen
WT
WT MeJA
L1
L1 MeJA
L2
L2 MeJA
L3
L3 MeJA
C
WT
Control
MeJA
amiR-VLG (L1)
Control
MeJA
D
Silique lenght (mm)
WT
WT MeJA
L1
L1 MeJA
L2
L2 MeJA
L3
L3 MeJA
E
WT
L1
L2
L3
Control
H_2O_2
F
Ratio Pistil/Stamen
WT
WT H_2O_2
L1
L1 H_2O_2
L2
L2 H_2O_2
L3
L3 H_2O_2
G
WT
Control
H_2O_2
amiR-VLG (L1)
Control
H_2O_2
H
Silique lenght (mm)
WT
WT H_2O_2
L1
L1 H_2O_2
L2
L2 H_2O_2
L3
L3 H_2O_2

Figure 5

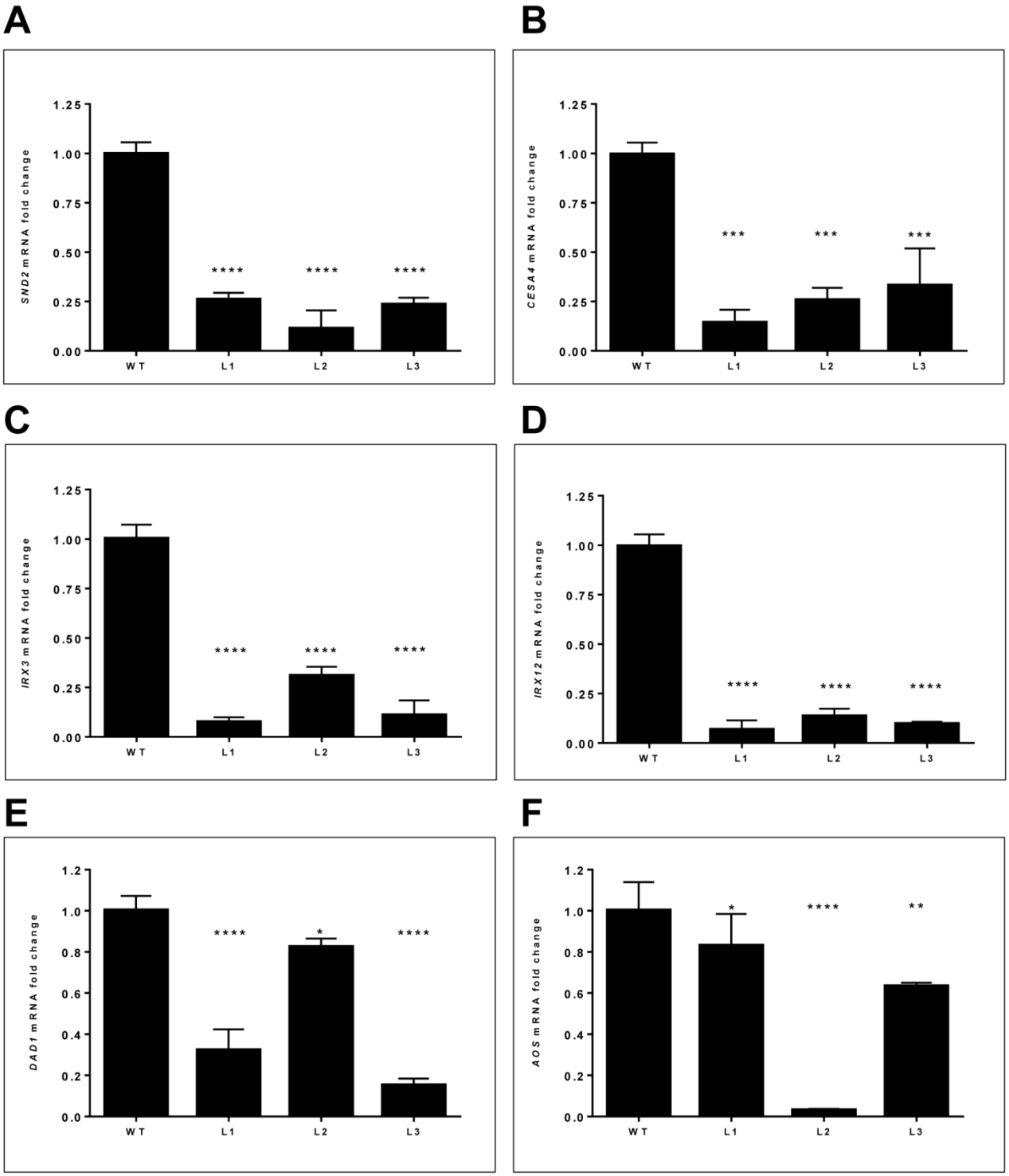
A
SND2 mRNA fold change
1.25
1.00
0.75
0.50
0.25
0.00
****
****
****
WT
L1
L2
L3
B
CESA4 mRNA fold change
1.25
1.00
0.75
0.50
0.25
0.00
***
***
***
WT
L1
L2
L3
C
IRX3 mRNA fold change
1.25
1.00
0.75
0.50
0.25
0.00
****
****
****
WT
L1
L2
L3
D
IRX12 mRNA fold change
1.25
1.00
0.75
0.50
0.25
0.00
****
****
****
WT
L1
L2
L3
E
DAD1 mRNA fold change
1.2
1.0
0.8
0.6
0.4
0.2
0.0
****
*
****
WT
L1
L2
L3
F
AOS mRNA fold change
1.2
1.0
0.8
0.6
0.4
0.2
0.0
*
****
**
WT
L1
L2
L3